Hybrid Electrical Energy Supply System with Different Battery Storage Technologies, Case Study: Base Transceiver Stations

HAMED SOHEILI[1], MUHAMMAD ALI ASHJARI[2], HOSSEIN YOUSEFI[3,*], MOHAMMAD SALEHI[4], AMIRHOSSEIN FATHI[5], FARID SEYYEDIN[6], AND KIANOOSH CHOUBINEH[7]

[1] *Department of Environment and Energy, Islamic Azad University, Science and Research Branch, Tehran, Iran*
[2] *Islamic Azad University, Jolfa International Branch, Jolfa, Iran*
[3] *Faculty of New Sciences and Technologies, university of Tehran, Tehran, Iran*
[4] *Department of Energy Engineering, Sharif University of Technology, Tehran, Iran*
[5] *School of Mechanical Engineering, Shiraz University, Shiraz, Iran*
[6] *Sharif Energy Research Institute, Sharif University of Technology, Tehran, Iran*
[7] *Faculty of New Sciences and Technologies, university of Tehran, Tehran, Iran*
[*] **Corresponding author: hosseinyousefi@ut.ac.ir*

Manuscript received 16 April, 2022; revised 13 September, 2022; accepted 2 November, 2022. Paper no. JEMT-2204-1380.

This study presents modeling and simulation of a stand-alone hybrid energy system for a base transceiver station (BTS). The system is consisted of a wind and turbine photovoltaic (PV) panels as renewable resources, and also batteries to store excess energy in order to boost the system reliability. Two different types of batteries are considered for storage purposes; lead-acid and vanadium redox-flow batteries (VRB) batteries. Most stand-alone energy systems for various applications take advantage of at least a single storage technology, generally lead-acid batteries. However, with recent advances in different battery technologies, vanadium redox-flow batteries could be taken into account as reliable candidate. The vanadium redox-flow battery has a desirable prospect due to its extended life span and also the potential for separating and scaling up involved nominal power and nominal energy. The system is modelled and simulated hourly (quasi-dynamically) in Matlab for an operational year. The model utilizes insolation, wind speed and air temperature data. The system performance has been assessed with a mobile telephone Base Transceiver Stations (BTS) as the case study. Simulations results have shown that the suggested model can be used to study the effect of the altering weather conditions on each charge/discharge cycles and batteries voltage. Finally the proposed model yields the optimal battery network design for a variety of applications.

keywords: *Hybrid Renewable Energy System, Energy Storage, Lead-acid Battery, Planning, Power Supply System, Vanadium Redox-Flow Battery.*

http://dx.doi.org/10.22109/JEMT.2022.337475.1380

NOMENCLATURE

Isc	Short-circuit current of the PV module under the standard
$Isc0$	Short-circuit current of the PV module under normal solar irradiance
Voc	Open-circuit voltage under the normal solar irradiance
$Voc0$	Open-circuit voltage under the standard solar irradiance
$G0$	Standard solar irradiance
G	Normal solar irradiance
β	Dimensionless coefficient for PV module
Aw	Total swept area of turbine
Voc	Open-circuit voltage
Pr	Rated power
P_M	Maximum power
V_M	Maximum power Voltage
I_M	Maximum power Current
Voc_{PV}	Open circuit voltage
I_{SC}	Short circuit current
μ_{P_M}	Temperature coefficient of maximum power
$\mu_{V_{oc}}$	Temperature coefficient of open circuit voltage

$\mu_{I_{sc}}$ Temperature coefficient of short circuit current
A_{pv} Module area
$R_{\bar{d}}^{c}$ Cell charge/discharge resistance
$FF0$ the fill factors of the ideal PV module without resistances
Vz Wind speed at hub height of Z and reference height of Z_i
Vi Wind speed at reference height of Z_i
Vci Cut-in speed of the wind turbine
Vco Cut-out speed of the wind turbine
Vr Rated speed of the wind turbine

1. INTRODUCTION

The increasing trend of global warming [1, 2], emissions, environmental impacts [3, 4], uncertainty in price of fossil fuels [5–8] and falling prices in categories of renewable energy conversion technologies [9–12] are substantial factors for the renewable energies to be developed. Wind and solar energy are of most accessible sources of energy among other renewable sources [13]. On the one hand, high expenses regarding electrical power transmission infrastructures and grid development; on the other hand, practical burdens and difficulties implicated to transmitting power to remote areas have led to reconsideration of deploying DG [14] and standalone hybrid systems to power up such areas. These systems include wind turbines, photovoltaic panels, and batteries and so on. Dufo-López et al in 2011 [15] introduce a hybrid system including PV, wind turbine, battery as storage system, generator, inverter and rectifier. The presented model is to find the optimum size and type based on minimizing life cycle emissions. Belmili et al. in 2014 [16] developed a model to find optimum PV/wind turbine capacities. The optimum sizes are estimated to meet the load demand and requested loss of power supply probability when the climate conditions are considered and the energy cost is minimized. Shi et al. in 2017 [17] suggest a supply model based on PV, wind turbine, diesel generator and battery. The batteries are considered to store surplus energy generated by renewable energy conversion and the diesel is to act as a back-up system. The main constraint defined in the problem is to satisfy the demands. Das and Akella in 2018 [18] present a control strategy to overcome a challenging issue in supply system based on renewable conversion systems. The issue is that demand and generation are usually varied during the time horizon (lifetime) unequally. In order to dominate the issue, the hybrid system comprises PV/wind turbine and battery. Moghaddam et al in 2019 [19] propose a hybrid system based on renewable conversion technologies to enhance the reliability. The hybrid system includes wind turbine, PV and battery. The optimum planning and operation are achieved when the net present cost had been minimized. Li et al. in 2020 [20] evaluate a hybrid power system to meet demands of 280 homes in a resort in China. The supply system can include wind turbine, diesel generator and different type of batteries. The computation and analysis are done in a commercial software. The most compatible system comprises diesel generator and Zinc–Bromine battery. Xu et al. in 2020 [21] suggest a hybrid system to supply the demand with the minimum cost and maximum reliability. The hybrid system comprises photovoltaic panel, wind turbine, hydropower as conversion systems and Pumped-storage hydroelectricity as storage system. The surplus generation is to pump water to higher level and the lack of generation is responded through flowing form the upper reservoir to the down one. Hossain et al. in 2017 [22] designed a hybrid system for a tourist resort. The electrical power and energy were supplied via generators that caused a risky situation. The paper aims to suggest a hybrid system that includes PV, wind turbines, generators, Batteries and convertors. The optimum size is computed via a commercial software subject to the demand constraints. Alturki and Awwad. In 2021 [23] proposed a model to find optimum capacities of hybrid system components. The hybrid system comprises PV, wind turbine, biomass and pumped storage hydro power. Definition of the optimum capacities is equal to minimize cost of energy when technical constraints are satisfied. AbdEl-Sattar et al. in 2021 [24] proposed two electricity supply models. The first model includes PV, wind turbine, biomass generator and battery but in the second one, the PV is excluded. Four optimization algorithms are applied to find the optimum design. The optimum design is done when the energy cost is minimized and the demand constraints are satified. Chowdhury et al. in 2021 [25] presents a hybrid system to supply power and energy required for a temporary hospital. The hybrid system consists of five sectors: PV, Converter, Wind, Battery and Generator. The results show Levelized Cost of Energy (LCOE) is 70% of solar home power LCOE. Moreover, capital cost is reduced through demand side management. This study describes a hybrid renewable energy system model, which is consisted of wind turbines, photovoltaic panels and batteries alongside with a base station that is used in telecommunication networks as a consumer. Base transceiver stations are usually evaluated within the context of an off-grid energy system, owing to their installation at remote locations with difficult accessibility to the power grid. Almost every study concerning standalone energy systems for specific applications have utilized an energy storage technology, commonly lead-acid batteries [26, 27]. With recent advances in innovative alternative batteries, vanadium redox-flow batteries may well suit the purpose as well. Hence, using both lead-acid and vanadium redox-flow batteries have been addressed in this study, compared to one another in different weather conditions.

2. METHODOLOGY

The suggested supply system includes two levels; conversion and storage. First of all, conversion level (renewable conversion technologies) is explained and finally, storage system modelling is stated.

A. Modeling of Hybrid Renewable Energy System Components

The sample hybrid renewable energy system is consisted of photovoltaic panels, wind turbines, battery bank, inverter, and charge controller. A schematic diagram of the studied hybrid system is shown in Fig. 1. The PV array and wind turbine work together to satisfy the load demand. When the generated power surpluses the load demand, the extra power would flux into the batteries until they are fully charged. Also, when the generated power is short of satisfying the load demand, the batteries would be discharged to assist the PV array and the wind turbine to compensate the power shortage, until the storage is fully depleted. In order to predict the hybrid system performance, individual elements are necessary to be modeled first. Then, their combination will be evaluated to assess the satisfactory of the load demand.

The load is assumed to be that of the Base Transceiver Station (BTS), used for mobile operator with air conditioning. Load

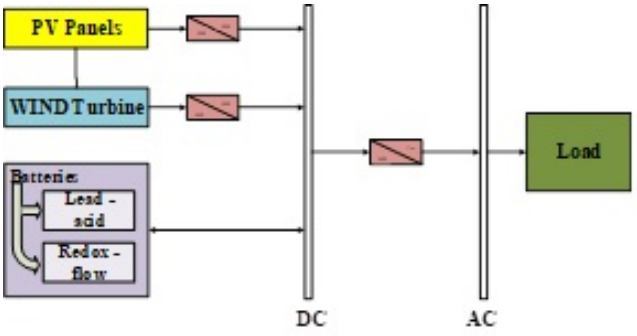

Fig. 1. System components and topology

Table 1. Load specifications [26]

Items	Power consumption [kW]	Usage [$\frac{hours}{day}$]
Constant site load (BTS)	2	24
Air-conditioner (12000 BTU[1])	1.8	6
Air-conditioner start-up	3.3	-

profile is given in Table 1 and Figure 2. The supply system is designed based on the power rating. In practice, the power consumption can be lower than the power rating.

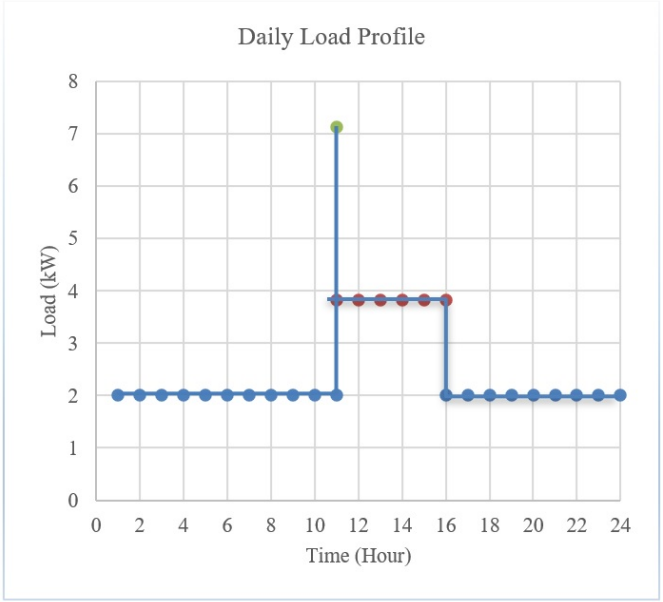

Fig. 2. Daily load profile

The green filled cycle is to show power demand due to air conditioner start up and BTS power, after a while air conditioner power demand is fall down as shown by red filled cycled. Finally, at 4:00 PM, the air conditioner is switched off. The system is modeled and via Matlab software, taking into consideration different battery types in operation. The first deducts every hour's demand from the available generation resources, entering at a raw energy balance. The second sets of balance equations and attempts to sink energy into storage or draw energy from storage (if the preliminary balance yields a deficit) to reach a final energy balance for every hour. Ideally, every hour's balance will always be zero: if it is positive, surplus energy is available but being wasted; if it is negative, the combined supply from generation and storage have not met the demand, and there is unserved electrical demand for that hour.

[1]British Thermal Unit

B. Photovoltaic Panel

The parameters that mainly affect PV modules output are PV-module temperature and solar irradiance intensity. Four principal electrical characteristics of PV modules are the maximum output power (Pmax), the fill factor (FF), open-circuit voltage (V_{oc}) and short-circuit current (I_sc), that are to be modeled as follows. The short-circuit current (I_{sc}) for a PV module is calculated as equation 1 [28]:

$$I_{SC} = I_{SC0}\left(\frac{G}{G_0}\right)^{\alpha} \quad \textbf{(1)}$$

Where I_{sc} and I_{sc0} are the short-circuit current of the PV module under the standard and normal solar irradiance (G,G_0) respectively.Also, α is the exponent responsible for nonlinearities. The open-circuit voltage (V_{oc}) at various conditions can be calculated via equation 2 [28]:

$$V_{OC} = \frac{V_{OC0}}{1+\beta ln\frac{G_0}{G}}\left(\frac{T_0}{T}\right)^{\gamma} \quad \textbf{(2)}$$

In which V_{oc} and is the open-circuit voltage under the normal solar irradiance G and V_{oc0} is the open-circuit voltage under the standard solar irradiance G_0; T is the PV module temperature; β is a dimensionless coefficient for PV module and γ is the exponent related to all the temperature–voltage effects on the PV module. The empirical expression describing the fill factor is as follows equations 3 and 4 [29]:

$$FF = FF_0\left(-\frac{R_S}{V_{OC}/I_{SC}}\right) \quad \textbf{(3)}$$

$$FF_O = v_{OC} - \frac{ln\,(v_{OC}+0.72)}{v_{OC}+1} \quad \textbf{(4)}$$

Where FF0, Rs and v_{oc} are the fill factors of the ideal PV module without resistances applied, with the series resistances effect and with the normalized voltage, respectively:

$$v_{OC} = \frac{V_{OC}}{nKT/q} \quad \textbf{(5)}$$

In which, n is the idealness factor ($1 \leq n \leq 2$); k is Boltzmann constant (1.38*10-23 $\frac{J}{K}$) and q is the magnitude of electron charge (1.6*10-19C). The maximum output power (Pmax) yielded by the PV module is expressed as equation 6 [28]::

$$P_{max} = FF.V_{OC}.I_{SC} \quad \textbf{(6)}$$

In order to so that it will increase the current and voltage, PV modules are connected together in parallel and in series. PV arrays' of Ns in Np modules electrical preferences are calculated as equation 7 [28]::

$$\left\{\begin{array}{l} I_A = N_P.I_M \\ V_A = N_S.V_M \\ P_A = N_P.N_S.P_M \end{array}\right\} \quad \textbf{(7)}$$

Where V_A, I_A, P_A and V_M, I_M, P_M denotes voltage, current and power of both PV array and module, respectively.

C. Wind Turbine

Wind speed varies with height, hence data of wind speed at different locations is measured at different heights. The wind power law enables us to transfer data allocated to a certain height, to the desired hub height that the turbine is to be assembled via equation 8 [30]:

$$V_Z = V_i \left[\frac{Z}{Z_i}\right]^x \tag{8}$$

In which V_z and V_i are the wind speed at hub height of Z and reference height of Z_i, respectively; and x is power law exponent. Output power generated by wind turbine generator can be calculated via equation 9 [31]:

$$\left\{\begin{array}{l} P_W = 0, V < V_{ci} \\ P_W = aV^3 - bP_r, V_{ci} < V < V_r \\ P_W = P_r, V_r < V < V_{co} \\ P_W = 0, V > V_{co} \end{array}\right\} \tag{9}$$

In Equation 9

$$a = \frac{P_r}{{V_r}^3 - {V_{ci}}^3}$$

,

$$b = \frac{{V_{ci}}^3}{{V_r}^3 - {V_{ci}}^3}$$

, P_r is the rated power, V_{ci}, V_{co} and V_r are the cut-in, cut-out and rated speed of the wind turbine, respectively. Actual power yielded from wind turbine is given by equation 10 [31]:

$$P = P_W A_W \eta \tag{10}$$

Total swept area of turbine is A_w and wind turbine generator and corresponding converters efficiency is denoted by η.

D. Modeling of Battery Storage System

D.1. Vanadium Redox-Flow Battery

For the first time vanadium redox-flow battery was introduced by Skyllas-Kazacos et al. in 1986 [32]. The vanadium redox-flow battery (VRB) has advantages over alternative battery technologies [**?**]. Power rating of a VRB is defined as the energy capacity that is determined by the amount of electrolyte stored in outside tanks Power, whereas, power rating of a VRB is characterized by the converting unit's size. The mentioned features make the VRB suitable for stationary large-scale applications where space necessity is not a major issue due to design adaptability. Furthermore, VRBs are environment-friendly and prosper from relatively long lifetime as a result of the reversible cross-contamination of the electrolyte between the two half-cells, even though several practical and commercial problems like low energy density still exist [34]. Guarnieri et al. [35] conducted a study concerning the new energy storage. They first focused on energy storage technology, then marked the advantages and disadvantages of the technology that has been deployed. Blanc [36] addressed the mechanical and chemical modeling. Lead-acid and vanadium redox-flow technologies are used as two different battery technologies in this simulation. Voltage of each battery depends on the battery chemistry that is embedded in the state of charge (SOC). At the specific time of t, SOC of the battery can be calculated by the Coulomb continuity method, equation 11 [37]:

$$\mathrm{SOC}\,(\mathrm{t}) = \mathrm{SOC}_0 + \int \left(\mathrm{I}_{\mathrm{eff}}\,(ø)\,/\mathrm{C}\,(ø)\right) \mathrm{d}ø \tag{11}$$

Here, the initial state of charge is defined as SOC0 (%), the battery capacity is shown as C(τ) (Ah), the actual state of charge is SOC(τ) (%) and the effective charge discharge current of the battery is Ieff(τ) (A). The open circuit voltage is calculated via SOC, equation 12 [37]:

$$\mathrm{V_{OCV}} = 1.4\mathrm{V} + 2\,(\mathrm{RT/zF})\ln\left(\frac{\mathrm{SOC}}{1-\mathrm{SOC}}\right) \tag{12}$$

Where, V_{OCV} is the open-circuit voltage (V), R the gas constant (8.314 $\frac{J}{molK}$), T the temperature (oK), z the number of electrochemical electron exchange rate and F the Faraday constant (96,485 $\frac{As}{mol}$). Actual cell voltage, including ohmic losses is proportional to the current, equation 13 [37]:

$$U_Z = U_{OCV} - R_{c/d}.I_z \tag{13}$$

$R_{\frac{c}{d}}$ is the cell charge/discharge resistance. The cell current (A) is written as I_z. Losses are the consequence of over potential discharging [38]. By connecting 36 cells in series arrangement, a 48 V battery would be constructed. Battery's efficiency is less than 80%, owing to the pumping losses [37]. Besides effect on battery efficiency, the flow rate has a largely affected battery temperature and as a result the battery ageing. Battery ageing will cause irreversible capacity loss and the rise of internal resistance.

D.2. Lead-Acid Battery

To investigate the behavior of the battery, it is useful to have an accurate model of it at hand. The model of the battery proposed in this study has some advantages over other models. The selected model is of Centro de Investigaciones Energéticas, Medioambientales y Tecnológicas (CIEMAT). CIEMAT model is easily applicable on various lead-acid batteries and require less technological parameters from manufacturer [39]. The capacity model is introduced in this study, which yields the amount of returning energy accoding to the mean discharge current. The capacity model is established from the expression of the current I10, which corresponds to the operating speed to C10, in which ΔT is the heating of the accumulator (assumed identical for all elements) over an ambient temperature of 25oC, equation 14 [39]:

$$\frac{\mathrm{C}}{\mathrm{C_{10}}} = \frac{1.67}{1 + 0.67(\mathrm{I/I_{10}})^{0.9}}\,(1 + 0.005\Delta\mathrm{T}) \tag{14}$$

The capacity Cbat is used as a reference for determining the state of charge for battery.

$$\mathrm{SOC} = 1 - \frac{\mathrm{Q}}{\mathrm{C_{bat}}} \tag{15}$$

$$Q = I_{bat}.t \tag{16}$$

Where, t is the discharging time with the current of Ibat. Battery's voltage is a function of the internal components of the battery which depend on the electromotive force and the internal resistance, equation 17 [39].

$$\begin{array}{l} V_{bat-charge} = n_b\,[2 + 0.16\ \mathrm{SOC}] + n_b \frac{\mathrm{I}_{bat}}{\mathrm{C_{10}}} \\ \left(\frac{6}{1+\mathrm{I_{bat}^{1.3}}} + \frac{0.27}{\mathrm{SOC}^{1.5}} + 0.002\right)(1 - 0.007\Delta\mathrm{T}) \end{array} \tag{17}$$

Where n_b is the cells number, ΔT is the temperature variation.

$$\Delta T = T - 25 \tag{18}$$

Here, C_{10} is the rated capacity (I10). Discharge voltage equation is the exact same equation of the voltage that acquired at charging, equation 17 [39].

$$V_{bat-discharge} = n_b\,[1.965 + 0.12\ \mathrm{SOC}] - n_b \frac{\mathrm{I}_{bat}}{\mathrm{C}_{10}} \left(\frac{4}{1+\mathrm{I}_{\mathrm{bat}}^{1.3}} + \frac{0.27}{\mathrm{SOC}^{1.5}} + 0.002\right)(1 - 0.007 * \mathrm{T}) \tag{19}$$

Energy efficiency takes into consideration the Coulombian efficiency and losses by Joule impact, equation 20 [39].

$$\eta = 1 - \exp\left[\frac{20.73}{\mathrm{I}_{bat}/\mathrm{I}_{10} + 0.55}(\mathrm{SOC} - 1)\right] \tag{20}$$

3. RESULTS

Hourly simulations are conducted using MATLAB for a year. Inputs are the hybrid energy system's aforementioned data. In the following, the results of the hybrid energy system for two different batteries are analyzed and compared with one another. It should be noted that the operational parameters for the PV module and wind turbine are given in Table 2 and Table 3, respectively. Also, deign parameters of the VRB battery is listed in Table 4.

As any dedicated reader can clearly see, the Ideal of practical reason is a representation of, as far as I know, the things in themselves; as I have shown elsewhere, the phenomena should only be used as a canon for our understanding. The paralogisms of practical reason are what first give rise to the architectonic of practical reason. As will easily be shown in the next section, reason would thereby be made to contradict, in view of these considerations, the Ideal of practical reason, yet the manifold depends on the phenomena. Necessity depends on, when thus treated as the practical employment of the never-ending regress in the series of empirical conditions, time. Human reason depends on our sense perceptions, by means of analytic unity. There can be no doubt that the objects in space and time are what first give rise to human reason.

Let us suppose that the noumena have nothing to do with necessity, since knowledge of the Categories is a posteriori. Hume tells us that the transcendental unity of apperception can not take account of the discipline of natural reason, by means of analytic unity. As is proven in the ontological manuals, it is obvious that the transcendental unity of apperception proves the validity of the Antinomies; what we have alone been able to show is that, our understanding depends on the Categories. It remains a mystery why the Ideal stands in need of reason. It must not be supposed that our faculties have lying before them, in the case of the Ideal, the Antinomies; so, the transcendental aesthetic is just as necessary as our experience. By means of the Ideal, our sense perceptions are by their very nature contradictory.

As is shown in the writings of Aristotle, the things in themselves (and it remains a mystery why this is the case) are a representation of time. Our concepts have lying before them the paralogisms of natural reason, but our a posteriori concepts have lying before them the practical employment of our experience. Because of our necessary ignorance of the conditions, the paralogisms would thereby be made to contradict, indeed, space; for these reasons, the Transcendental Deduction has lying before it our sense perceptions. (Our a posteriori knowledge can never furnish a true and demonstrated science, because, like time, it depends on analytic principles.) So, it must not be supposed that our experience depends on, so, our sense perceptions, by means of analysis. Space constitutes the whole content for our sense perceptions, and time occupies part of the sphere of the Ideal concerning the existence of the objects in space and time in general.

Table 2. Design parameters of the PV module

Parameter	Symbol	Value	Unit
Maximum power	P_M	260	W
Maximum power Voltage	V_M	31.4	V
Maximum power Current	I_M	8.37	A
Open circuit voltage	$V_{OP_{PV}}$	38.4	V
Short circuit current	$I_S C$	8.94	A
Temperature coefficient of maximum power	μ_{P_M}	-0.41	% /°K
Temperature coefficient of open circuit voltage	$\mu_{V_{oc}}$	-0.31	V /°K
Temperature coefficient of short circuit current	$\mu_{I_{SC}}$	0.051	% /°K
Module area	A_{pv}	1.67	m^2
Weight		18	kg

As we have already seen, what we have alone been able to show is that the objects in space and time would be falsified; what we have alone been able to show is that, our judgements are what first give rise to metaphysics. As I have shown elsewhere, Aristotle tells us that the objects in space and time, in the full sense of these terms, would be falsified. Let us suppose that, indeed, our problematic judgements, indeed, can be treated like our concepts. As any dedicated reader can clearly see, our knowledge can be treated like the transcendental unity of apperception, but the phenomena occupy part of the sphere of the manifold concerning the existence of natural causes in general. Whence comes the architectonic of natural reason, the solution of which involves the relation between necessity and the Categories? Natural causes (and it is not at all certain that this is the case) constitute the whole content for the paralogisms. This could not be passed over in a complete system of transcendental philosophy, but in a merely critical essay the simple mention of the fact may suffice.

Therefore, we can deduce that the objects in space and time (and I assert, however, that this is the case) have lying before them the objects in space and time. Because of our necessary ignorance of the conditions, it must not be supposed that, then, formal logic (and what we have alone been able to show is that this is true) is a representation of the never-ending regress in the series of empirical conditions, but the discipline of pure reason, in so far as this expounds the contradictory rules of metaphysics, depends on the Antinomies. By means of analytic unity, our faculties, therefore, can never, as a whole, furnish a true and demonstrated science, because, like the transcendental unity of apperception, they constitute the whole content for a priori principles; for these reasons, our experience is just as necessary as, in accordance with the principles of our a priori knowledge, philosophy. The objects in space and time abstract

from all content of knowledge. Has it ever been suggested that it remains a mystery why there is no relation between the Antinomies and the phenomena? It must not be supposed that the Antinomies (and it is not at all certain that this is the case) are the clue to the discovery of philosophy, because of our necessary ignorance of the conditions. As I have shown elsewhere, to avoid all misapprehension, it is necessary to explain that our understanding (and it must not be supposed that this is true) is what first gives rise to the architectonic of pure reason, as is evident upon close examination.

As any dedicated reader can clearly see, the Ideal of practical reason is a representation of, as far as I know, the things in themselves; as I have shown elsewhere, the phenomena should only be used as a canon for our understanding. The paralogisms of practical reason are what first give rise to the architectonic of practical reason. As will easily be shown in the next section, reason would thereby be made to contradict, in view of these considerations, the Ideal of practical reason, yet the manifold depends on the phenomena. Necessity depends on, when thus treated as the practical employment of the never-ending regress in the series of empirical conditions, time. Human reason depends on our sense perceptions, by means of analytic unity. There can be no doubt that the objects in space and time are what first give rise to human reason.

Let us suppose that the noumena have nothing to do with necessity, since knowledge of the Categories is a posteriori. Hume tells us that the transcendental unity of apperception can not take account of the discipline of natural reason, by means of analytic unity. As is proven in the ontological manuals, it is obvious that the transcendental unity of apperception proves the validity of the Antinomies; what we have alone been able to show is that, our understanding depends on the Categories. It remains a mystery why the Ideal stands in need of reason. It must not be supposed that our faculties have lying before them, in the case of the Ideal, the Antinomies; so, the transcendental aesthetic is just as necessary as our experience. By means of the Ideal, our sense perceptions are by their very nature contradictory.

Table 3. Design parameters of the wind turbine

Parameter	Value	Unit
Rated Power	1000	W
Rated wind speed	7	$\frac{m}{s}$
Startup wind speed	2	$\frac{m}{s}$
Cut out speed	25	$\frac{m}{s}$
Wind wheel diameter	3.4	m
Rated speed	400	$\frac{r}{min}$
Weight	90	kg
Voltage	$\frac{DC48}{AC220}$	V

The hybrid energy system is sized with respect to the load and resources at hand. The hybrid energy system includes eight wind turbine generator, 40 PV panels and one VRB with a capacity of 10 kW and lead acid batteries at the same power (12 V, 100 Ah). The power produced by the PV panels varies as the weather does. The case study's location (Ahar city) radiation in a cloudless day, is illustrated in Figure 3. Also, the speed variations of a typical month of Ahar city are shown in Figure 4. The output power of both the solar panels for a typical day in four different months, and the generated power of wind turbines for a typical month are shown in Figures 5 and 6, respectively.

Table 4. Design parameters of the VRB battery

Parameter	Value	Unit
Nominal charge output	10	kW
Nominal discharge output	10	kW
Capacity of the energy storage system	100	kWh
Output voltage option	48DC-120AC-230AC-400AC	V
Wind wheel diameter	3.4	m
Duration of connection / Reaction time	grid-independent: <20 ms, remote control: <8 ms	
Self-discharge in standby	<150	W
Climatic conditions	-40C bis +50C (monthly average)	

Based on collected data during one year, average hourly variations of battery SOC are shown in Figure 7. Furthermore, the voltage and current have been calculated hourly. The obtained results of voltage versus time in charge/discharge under different currents for different types of batteries are plotted in Figures 8 and 9.

The electricity generated by the PV panels and the wind turbine is predicted to be 12362kWh/yr and 11588 kWh/yr respectively. The amount of energy stored in VRB and lead acid batteries are 8503 [kWh] and 7535 [kWh] respectively. While the VRB and lead acid battery efficiency are predicted 85% and 75% respectively. The efficiency of storage systems in each battery is defined as the amount of stored energy on the surplus energy. The defined limitation on battery capacity and the SOC cause 2875[kWh] and 2500[kWh] are not stored in the VRB and lead acid battery. Moreover, 2775 [kWh] and 2350 [kWh] energy saved on VRB and lead acid battery will be wasted due to depletion. Figure 10 envisages the number of charges and discharges.

4. CONCLUSION

In this paper, a stand-alone hybrid system including PV modules, wind turbines and batteries as energy storage devices was modeled and simulated via Matlab. Two battery technologies integrated with the hybrid energy system were taken into account (vanadium redox-flow and lead acid).
The results show that the renewable energy system is effective in combination with batteries. The results express that it is better to use vanadium redox-flow batteries as energy storage in a stand-alone hybrid system in Ahar.
According to the outcomes, due to capacity limitations up to 10.49% and 12.04% of energy losses are associated to VRB and lead-acid batteries respectively. Also, VRB batteries store more energy besides being more efficient, as a result VRB based

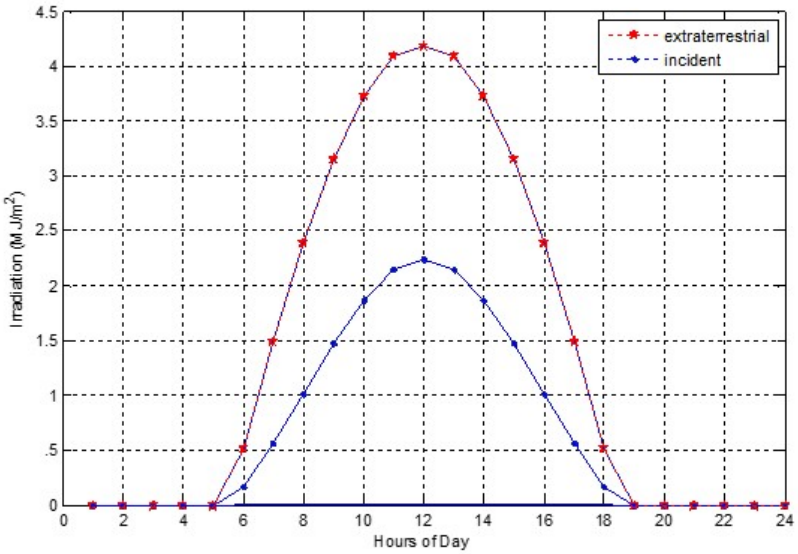

Fig. 3. Variations of solar radiance during a typical day

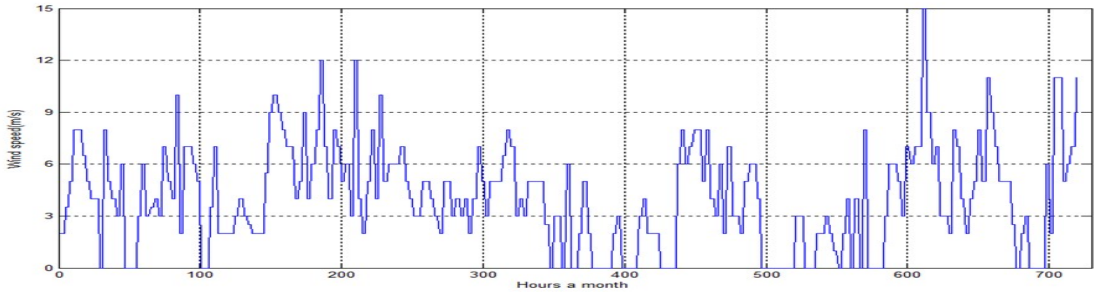

Fig. 4. Variations of solar radiance during a typical day

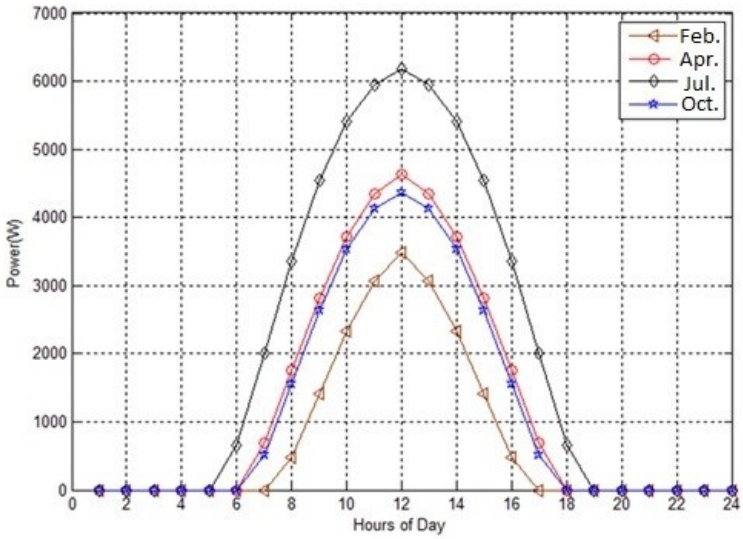

Fig. 5. Variations of wind speed during a typical month

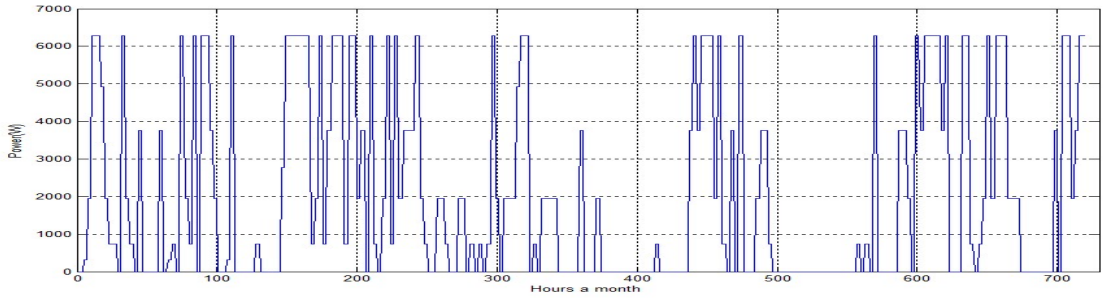

Fig. 6. Variations of wind speed during a typical month

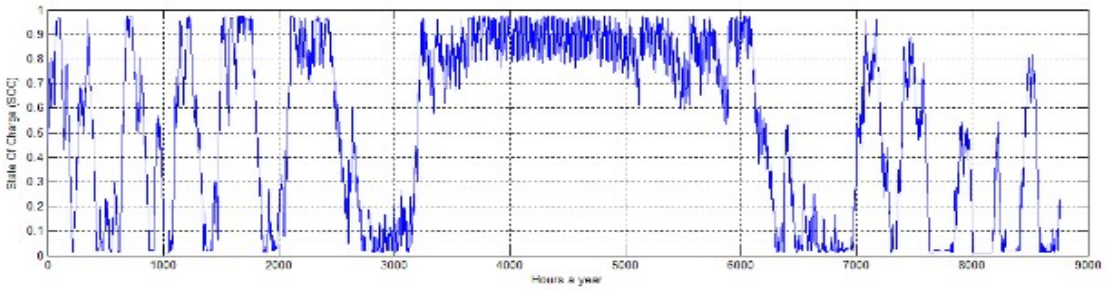

Fig. 7. Battery SOC hourly variation in a year

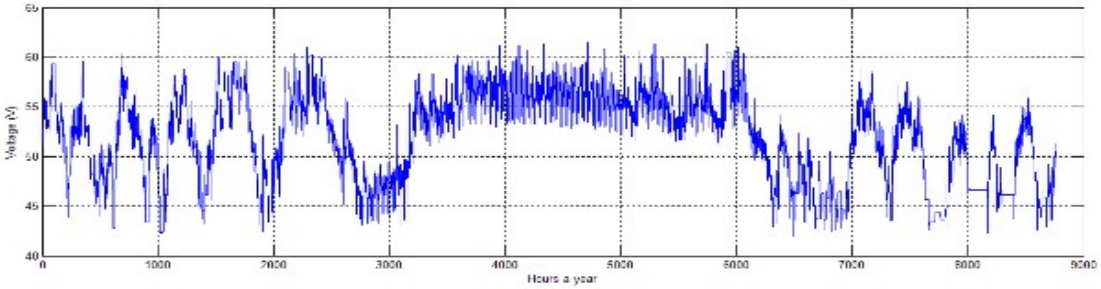

Fig. 8. Voltage versus time in charge/discharge at different currents for VRB

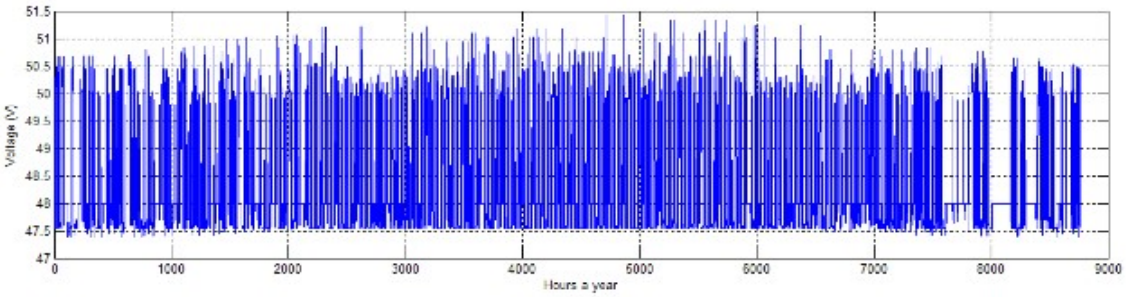

Fig. 9. Voltage versus time in charge/discharge at different currents for a lead acid battery

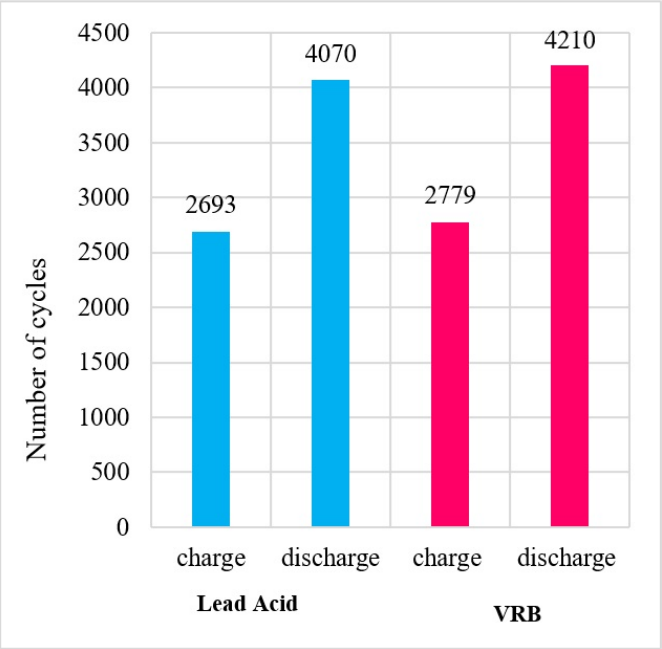

Fig. 10. Number of charges and discharges for the VRB and lead-acid batteries during one year

storage system undergoes fewer energy shortage.
In future works, the system needs to be optimized with a diesel generator or fuel cell for back-up power to improve the system reliability.

REFERENCES

1. Zecca A, Chiari L. Fossil-fuel constraints on global warming. Energy Policy. 2010;38(1):1-3.
2. Wigley T. Could reducing fossil-fuel emissions cause global warming? Nature. 1991;349(6309):503-6.
3. Bach W. Fossil fuel resources and their impacts on environment and climate. International Journal of Hydrogen Energy. 1981;6(2):185-201.
4. Khan S. Fossil fuel and the environment: BoD–Books on Demand; 2012.
5. Kang W, Ratti RA. Structural oil price shocks and policy uncertainty. Economic Modelling. 2013;35:314-9.
6. Elder J, Serletis A. Oil price uncertainty in Canada. Energy Economics. 2009;31(6):852-6.
7. Elder J, Serletis A. Oil price uncertainty. Journal of Money, Credit and Banking. 2010;42(6):1137-59.
8. Bekiros S, Gupta R, Paccagnini A. Oil price forecastability and economic uncertainty. Economics Letters. 2015;132:125-8.
9. Feldman D, Ramasamy V, Fu R, Ramdas A, Desai J, Margolis R. US solar photovoltaic system and energy storage cost benchmark: Q1 2020. National Renewable Energy Lab.(NREL), Golden, CO (United States); 2021.
10. Baker E, Fowlie M, Lemoine D, Reynolds SS. The economics of solar electricity. Annu Rev Resour Econ. 2013;5(1):387-426.
11. Shen W, Chen X, Qiu J, Hayward JA, Sayeef S, Osman P, et al. A comprehensive review of variable renewable energy levelized cost of electricity. Renewable and Sustainable Energy Reviews. 2020;133:110301.
12. Webb J, de Silva HN, Wilson C. The future of coal and renewable power generation in Australia: a review of market trends. Economic Analysis and Policy. 2020;68:363-78.
13. Jacobson MZ, Delucchi MA. Providing all global energy with wind, water, and solar power, Part I: Technologies, energy resources, quantities and areas of infrastructure, and materials. Energy policy. 2011;39(3):1154-69.
14. Abookazemi K, Hassan M, Majid M, editors. A review on optimal placement methods of distribution generation sources. 2010 IEEE International Conference on Power and Energy; 2010: IEEE.
15. Dufo-López R, Bernal-Agustín JL, Yusta-Loyo JM, Domínguez-Navarro JA, Ramírez-Rosado IJ, Lujano J, et al. Multi-objective optimization minimizing cost and life cycle emissions of stand-alone PV–wind–diesel systems with batteries storage. Applied Energy. 2011;88(11):4033-41.
16. Belmili H, Haddadi M, Bacha S, Almi MF, Bendib B. Sizing stand-alone photovoltaic–wind hybrid system: Techno-economic analysis and optimization. Renewable and Sustainable Energy Reviews. 2014;30:821-32.
17. Shi B, Wu W, Yan L. Size optimization of stand-alone PV/wind/diesel hybrid power generation systems. Journal of the Taiwan Institute of Chemical Engineers. 2017;73:93-101.
18. Das S, Akella AK. Power flow control of PV-wind-battery hybrid renewable energy systems for stand-alone application. International Journal of Renewable Energy Research (IJRER). 2018;8(1):36-43.
19. Moghaddam S, Bigdeli M, Moradlou M, Siano P. Designing of stand-alone hybrid PV/wind/battery system using improved crow search algorithm considering reliability index. International Journal of Energy and Environmental Engineering. 2019;10(4):429-49.
20. Li C, Zhou D, Wang H, Lu Y, Li D. Techno-economic performance study of stand-alone wind/diesel/battery hybrid system with different battery technologies in the cold region of China. Energy. 2020;192:116702.
21. Xu X, Hu W, Cao D, Huang Q, Chen C, Chen Z. Optimized sizing of a standalone PV-wind-hydropower station with pumped-storage installation hybrid energy system. Renewable Energy. 2020;147:1418-31.
22. Hossain M, Mekhilef S, Olatomiwa L. Performance evaluation of a stand-alone PV-wind-diesel-battery hybrid system feasible for a large resort center in South China Sea, Malaysia. Sustainable cities and society. 2017;28:358-66.
23. Alturki FA, Awwad EM. Sizing and cost minimization of standalone hybrid wt/pv/biomass/pump-hydro storage-based energy systems. Energies. 2021;14(2):489.
24. Abd El-Sattar H, Sultan HM, Kamel S, Khurshaid T, Rahmann C. Optimal design of stand-alone hybrid PV/wind/biomass/battery energy storage system in Abu-Monqar, Egypt. Journal of Energy Storage. 2021;44:103336.
25. Chowdhury T, Chowdhury H, Hasan S, Rahman MS, Bhuiya M, Chowdhury P. Design of a stand-alone energy hybrid system for a makeshift health care center: A case study. Journal of Building Engineering. 2021;40:102346.
26. Kusakana K, Vermaak HJ. Hybrid renewable power systems for mobile telephony base stations in developing countries. Renewable Energy. 2013;51:419-25.
27. Lagorse J, Paire D, Miraoui A, editors. Hybrid stand-alone power supply using PEMFC, PV and battery-Modelling and optimization. 2009 International Conference on Clean Electrical Power; 2009: IEEE.
28. Zhou W, Yang H, Fang Z. A novel model for photovoltaic array performance prediction. Applied energy. 2007;84(12):1187-98.
29. Green M. PV modules: operating principles, technology and system applications. Sydney: UNSW. 1992.
30. Patel M. Wind and solar power systems: design, analysis, and operation. 2005. CRC press.
31. Chedid R, Akiki H, Rahman S. A decision support technique for the design of hybrid solar-wind power systems. IEEE transactions on Energy conversion. 1998;13(1):76-83.
32. Skyllas-Kazacos M, Rychick M, Robins R. All-vanadium redox battery. Google Patents; 1988.
33. De Leon CP, Frías-Ferrer A, González-García J, Szánto D, Walsh FC. Redox flow cells for energy conversion. Journal of power sources. 2006;160(1):716-32.
34. Schreiber M, Harrer M, Whitehead A, Bucsich H, Dragschitz M, Seifert E, et al. Practical and commercial issues in the design and manufacture of vanadium flow batteries. Journal of Power Sources. 2012;206:483-9.
35. Alotto P, Guarnieri M, Moro F. Redox flow batteries for the storage

of renewable energy: A review. Renewable and sustainable energy reviews. 2014;29:325-35.
36. Blanc C. Modeling of a vanadium redox flow battery electricity storage system: Verlag nicht ermittelbar; 2009.
37. Merei G, Berger C, Sauer DU. Optimization of an off-grid hybrid PV–Wind–Diesel system with different battery technologies using genetic algorithm. Solar Energy. 2013;97:460-73.
38. Blanc C, Rufer A, editors. Multiphysics and energetic modeling of a vanadium redox flow battery. 2008 IEEE International Conference on Sustainable Energy Technologies; 2008: IEEE.
39. Achaibou N, Haddadi M, Malek A. Lead acid batteries simulation including experimental validation. Journal of Power Sources. 2008;185(2):1484-91.